RSC Advances

PAPER

View Article Online
View Journal | View Issue

Cite this: *RSC Adv.*, 2024, **14**, 27644

Evaluating layer contributions and salt coating effects on mask performance†

Sumin Han,[a] Caitlyn Maliksi,[a] Euna Oh,[a] Surjith Kumaran,[a] Kyu Hyoung Lee,[b] Dae-Hong Ko[b] and Hyo-Jick Choi*[a]

The impact of respiratory diseases is vast and multifaceted, affecting individuals, healthcare systems, and global economies. In response to the spread of respiratory pathogens, masks and respirators have become pivotal, demonstrating their capability to mitigate transmission. However, the limitations of conventional face masks or respirators, such as their single-use nature, environmental impact, and the risk of contact-based transmission, have accelerated the development of antimicrobial masks. Designing effective antimicrobial masks requires a deep understanding of the properties of each layer and the identification of an optimal configuration to enhance their protective efficiency. In this study, we investigated the filtration performance, including filtration efficiency and breathability, of individual layers in conventional 3-ply masks and stacked spunbond (SB) fabrics with and without salt coating, under both dry and wet fabric conditions. We aimed to elucidate the filtration efficiency of each mask layer with respect to particle size and type (NaCl aerosols, DOP aerosols), with particular focus on the impact of salt-coated SB fabric and its application. While bare fabrics showed a decrease in filtration efficiency with increased wetness, salt-coated fabrics exhibited enhanced filtration efficiency. Importantly, evaluating the efficacy of a stack comprised of salt-coated SB fabrics across diverse antimicrobial respiratory devices highlighted its efficacy as both the outermost layer in a 3-ply mask and as a mask covering (*i.e.*, a supplementary layer over a mask or respirator). This investigation not only emphasizes the significance of salt-coated antimicrobial technology in mitigating disease transmission but also offers a practical approach for adeptly implementing this technology in respiratory protection devices.

Received 23rd June 2024
Accepted 28th August 2024

DOI: 10.1039/d4ra04581e

rsc.li/rsc-advances

1. Introduction

During pandemics and epidemics, the effectiveness of masks has been well-documented, with studies showing a 70–79% reduction in infection rates.[1–3] However, the conventional masks have limitations mainly due to the disposable nature of masks. To maintain filtration efficiency and reduce the risk of pathogen transmission through surface contamination, it is recommended that surgical masks be replaced immediately if they become wet, and at least every four hours under normal use.[4] The environmental impact of disposable masks is also a significant concern, as discarded masks can break down into microplastic fibers smaller than 5 mm, which can enter waterways and disrupt ecosystems.[5] This continuous cycle of demand, use, and environmental degradation underscores the urgent need for reusable antimicrobial masks that can protect public health while minimizing ecological harm.

The antimicrobial masks should be designed to fulfill multiple criteria, including non-toxicity, rapid pathogen inactivation, and a pathogen non-specific antimicrobial effect, prevention of contact transmission, and ease of scale-up.[6] Moreover, the masks should conform to guidelines such as filtration efficiency (see ESI Table S1† for international standards). To satisfy all the requirements, selecting appropriate functionalization strategy of antimicrobial material is crucial (*e.g.*, encapsulation in fiber, fiber surface adsorption, chemical functionalization on fiber, crosslinked antimicrobial coating, loading into fiber coating, and functionalization on fiber coating).[7] Surgical masks and respirators typically consist of 3 or 4 layers, including the outermost (O), middle (M), and inner (I) layers. The outermost spunbond polypropylene (SB PP) layer acts as a physical barrier to prevent contamination of the middle layer, which serves as the main filter capturing most particles. The inner layer that directly contacts with face supports the middle layer.[8] When selecting which layer to treat with antibacterial agents, it is important to consider the type

[a]*Department of Chemical and Materials Engineering, University of Alberta, Edmonton, AB T6G 1H9, Canada. E-mail: hyojick@ualberta.ca*

[b]*Department of Materials Science and Engineering, Yonsei University, Seoul 03722, Republic of Korea*

† Electronic supplementary information (ESI) available: Breath resistance and filtration efficiency standards; particle size-dependent filtration efficiency of single bare fabrics and salt-coated fabric only conditions; filter performance of bare and salt-coated fabrics with different stacking sequences; filtration efficiency of wet I × 3 and I_{NaCl} × 3 as a cover and an outer layer of the 3-ply mask. See DOI: https://doi.org/10.1039/d4ra04581e

and size of the pathogenic particles and choose a functionalization strategy that meets all the necessary performance requirements.

Particle-dependent filtration efficiency can be used for testing the performance of the designed masks. The main filtration mechanism depends on particle size; for instance, sedimentation and inertial impaction are mainly observed for large particles (1–10 μm), while interception and diffusion are significant for particles ranging from 0.1–1 μm, and electrostatic attraction is crucial for particles smaller than 300 nm.[9] Understanding size-dependent filtration efficiency enables the identification of primary mechanisms for capturing infectious aerosols/droplets carrying viruses and bacteria, as well as the quantitative assessment of each layer's role in pathogen capture. The predominant size of aerosols or droplets generated varies depending on the nature of human activities; talking (35–150 μm), coughing (45–200 μm), resting (<0.57–0.71 μm), and manual rubbing of mask fabric (0.3–2 μm).[10–13] Given these variations, different filtration mechanisms are required to effectively capture particles during different activities. For example, in healthcare settings or during conversations, large particles are more common, and thus masks need to have high filtration efficiency for these larger particles. This understanding is crucial for determining which mask layers should be treated with antimicrobial agents to target specific modes of disease transmission.

Evaluation of environmental conditions and surface treatments is critical when characterizing the performance of filtration masks. In practical applications, masks frequently encounter humid environments, particularly when worn for extended durations or in colder climates. The humidity generated primarily from exhaled breath can significantly influence the filtration efficiency of masks. Typically, exhaled breath humidity ranges from 41.9–91% at temperature of 31.4–35.4 °C.[14] Studies indicate that prolonged mask usage increases internal humidity from approximately 61.6 ± 11.2% to 88.5 ± 11.7%.[15] Many meltblown (MB) filters of masks depend on electrostatically charged fibers to enhance particle capture. However, previous reports have demonstrated that exposure to humidity can significantly reduce this electrostatic charge, thereby compromising the filtration efficiency of masks.[16] For instance, polypropylene (PP) filters have been shown to lose 56.9% to 61.2% of their electric potential after 48 hours of exposure to 90% RH.[17] Besides, ethanol and steam treatment on N95 masks led to a reduction in filtration efficiency to 77% and 50%, respectively, although this efficiency can be partially restored to 86% following recharging.[18] Given that electrostatic charge can account for about 9–69% of the filtration efficiency of masks, the degradation of this charge due to humidity is of considerable importance.[17–19] Therefore, incorporating considerations of wetness and humidity into the assessment of filtration efficiency is important for accurate evaluations.

To effectively control the spread of infectious diseases, various antimicrobial materials, such as metallic nanoparticles, synthetic chemicals, and natural extracts, have been applied to masks. However, these materials often present limitations, including challenges in application, potential toxicity, and/or low antimicrobial activity.[20–22] Designing effective antimicrobial masks requires meeting several key criteria: rapid inactivation, broad-spectrum (non-specific) pathogen inactivation, cost-effectiveness, and safety. Overcoming these challenges necessitates the careful selection of optimal materials and coating or functionalization methods to achieve rapid, non-specific pathogen inactivation without compromising safety. In response to these needs, we have developed salt-coated fabrics that inactivate pathogens through a process of salt recrystallization, which occurs when pathogen-laden aerosols/droplets come into contact with the salt-coated fabric surface.

Previous studies have demonstrated the rapid antimicrobial activity of salt-coated fabrics against diverse pathogens, including bacteria (*e.g.*, *E. coli*, *K. pneumonia*, *S. pyogenes*, *P. aeruginosa*, and MRSA) and viruses (*e.g.*, influenza viruses and coronaviruses), and inactivation mechanism.[23] It was found that pathogen inactivation efficiency is related to the amount of salt and salt type (NaCl, KCl, and K_2SO_4).[7,23] However, their filter performance, specifically filtration efficiency and pressure drop, was not fully characterized in relation to the quantity of salt and moisture. Hence, the primary objective of this paper is to examine the mask performance of salt-coated fabrics with different salt amount (5, 9, and 13 mg cm^{-2}) and salt type (NaCl, KCl, and K_2SO_4). The results was compared with those of bare filters to identify the effects of salt coating on mask performance and the functionalization strategy. This study can contribute to reveal (1) particle-size dependent filtration mechanism of different configuration of mask fabrics, (2) effects of salt coating on mask performance and optimization of salt-coated fabric configuration, and (3) the effects of wetness on filtration efficiency and breathability.

2. Results and discussion

2.1 Filter performance of bare fabrics

Filtration efficiency and breathability are critical factors in accessing the performance of surgical masks and respirators (see Table S1† for detailed guidelines). Filtration efficiency was tested using two different types of aerosols: 5% NaCl and dioctyl phthalate (DOP), following NIOSH 42CFR84 standards. NaCl aerosols are hydrophilic because the Na^+ and Cl^- ions attract water molecules through ion–dipole interactions. This charged ions enables them to interact with the charged fibers of a filter through electrostatic attraction. In contrast, DOP is hydrophobic and non-charging due to its long non-polar alkyl chain, making its capture in filters rely more on mechanical processes such as interception, impaction, and diffusion, rather than on electrostatic interactions.[24]

The main objective was to assess the performance of individual layer (SB outer: O, MB middle: M, and SB inner: I) within a 3-ply mask (O/M/I) and stacked SB PP fabrics. Additionally, the study aimed to evaluate the performance of masks in different configurations, such as stacked SB fabrics used as the outer layer of a 3-ply mask or as a mask covering. To this end, the following conditions were tested: single layers (O, M, and I); stacked SB inner layers (2, 3, 4, and 5 stacked inner layers; a stack of *n* inner layers is abbreviated as I × *n*); 3-ply masks (O × 1/M × 1/I × 1),

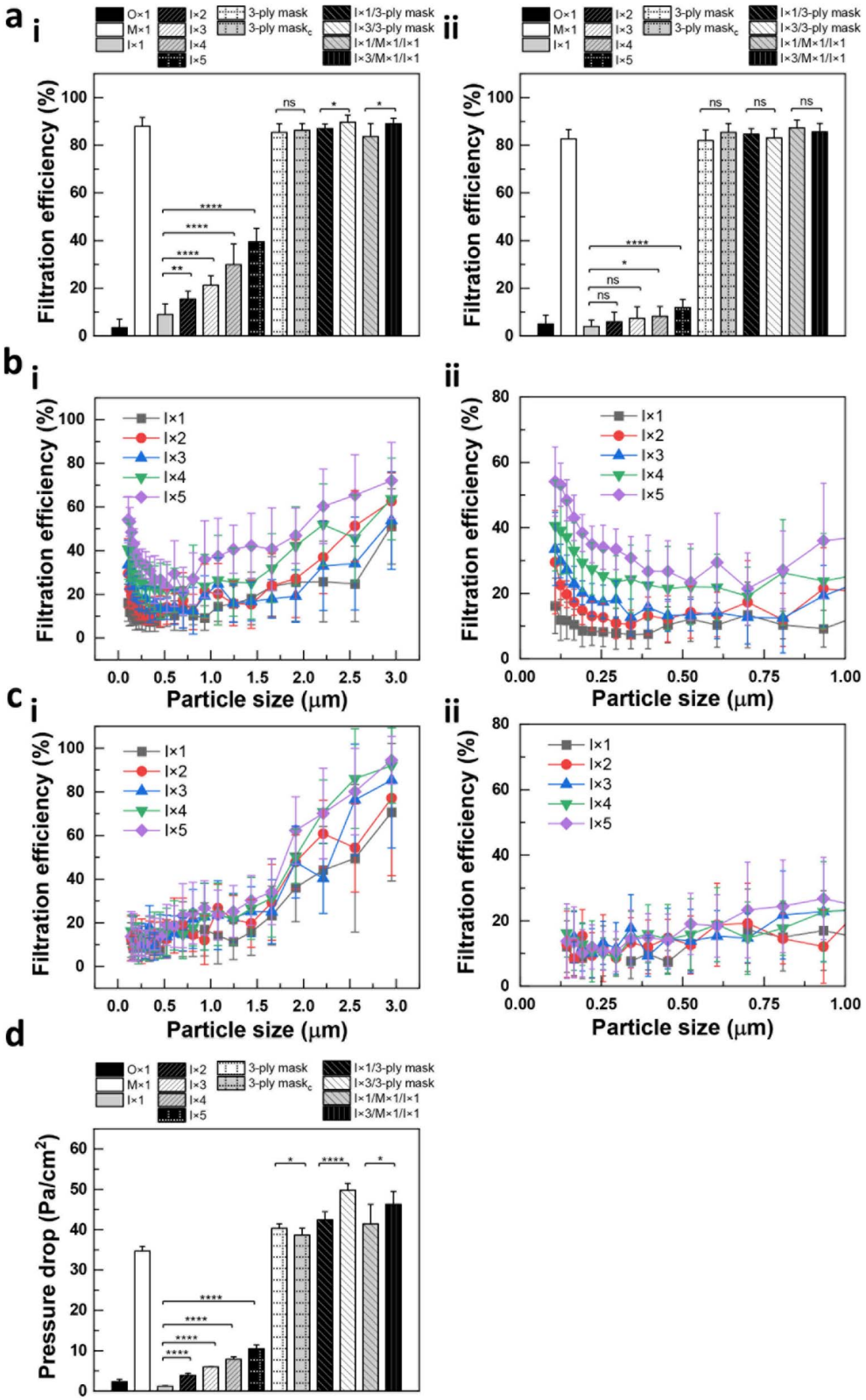

Fig. 1 Filter performance of bare fabrics. Filtration efficiency and breathability were performed according to NIOSH 42CFR84 and ASTM F2100-19e1 standards, respectively. (a) Overall filtration efficiency of bare fabrics tested with 5% NaCl aerosol (i) and DOP aerosol (ii). ($n = 10–21$ for a(i) and 13–24 for a(ii), mean ± SD). (b and c) Particle size-dependent filtration efficiency tested with 5% NaCl aerosols (b) and DOP aerosols (c) (i: filtration efficiency of bare fabrics and ii: zoomed-in filtration efficiency of the bare fabrics). ($n = 7–21$ for b and 9–24 for c, mean ± SD). (d) Breathability of bare fabrics with different stacking sequences ($n = 9–12$, mean ± SD). For all panels: ns, $P > 0.05$; *, $P < 0.05$; **, $P < 0.01$ and ****, $P < 0.0001$ by one-way ANOVA. The obtained fabrics were labelled as $\text{Fabric}_{\text{Salt}} \times \#_{\text{Amount}}$. 'Fabric' indicates PP fabric type (I, M, O); 'Salt' the coating (T20, NaCl, KCl, K_2SO_4); '#' the number of layers (1–5); 'Amount' the coating weight (5, 9, 13 mg cm^{-2}). Bare fabrics are "Fabric × #", '#' being the layer count. The '/' symbol shows layer order, 'A/B' means A over B.

including both intact and reassembled masks (referred to as recombined 3-ply masks, *i.e.* 3-ply mask$_c$); and configurations where single or stacked inner layers were used as a mask cover (*i.e.*, I × 1/3-ply mask and I × 3/3-ply mask) or as an outer layer of a mask (I × 1/M × 1/I × 1 and I × 3/M × 1/I × 1).

Our findings revealed that the middle layer exhibited the highest filtration efficiency, with an average of 88 ± 4% for 5% NaCl aerosols and 83 ± 4% for DOP aerosols (Fig. 1a(i,ii)). In addition, filtration efficiency increased with the number of stacked inner layers in both NaCl and DOP aerosols (GLM, $P = 0.0221$ for I × 1 and $P < 0.0001$ for I × 2, I × 3, I × 4, I × 5). This trend was more pronounced for NaCl aerosols (Fig. 1a(i)) compared to DOP aerosols (Fig. 1a(ii)): I × 1 (NaCl: 9 ± 4%, DOP: 4 ± 3%; *t*-test, $P = 0.0013$), I × 2 (NaCl: 15 ± 3%, DOP: 6 ± 4%; *t*-test, $P < 0.0001$), I × 3 (NaCl: 21 ± 4%, DOP: 7 ± 5%; *t*-test, $P < 0.0001$), I × 4 (NaCl: 30 ± 9%, DOP: 8 ± 4%; *t*-test, $P < 0.0001$), and I × 5 (NaCl: 40 ± 5%, DOP: 12 ± 3%; *t*-test, $P < 0.0001$). This significant increase in filtration efficiency with the number of SB fabrics contrasts with the relatively low efficiency of a single SB PP fabric (used as either inner or outer layers of a 3-ply mask), suggesting that stacked SB fabrics could be effectively used in the design of 3-ply masks or as mask coverings to protect against biological contaminants in aqueous mediums. When comparing intact and reassembled 3-ply masks (3-ply mask *vs.* 3-ply mask$_c$), there was no significant difference in filtration efficiency for both NaCl and DOP aerosols (*t*-test, $P = 0.3439$ and $P = 0.0707$, respectively). This result suggests greater flexibility in the fabrication of antimicrobial face masks, as individual layers can be functionalized and stacked without compromising filtration efficiency.

To further assess the impact of the use of stacked SB fabrics, the filtration efficiency of two configurations, I × 3/3-ply masks (with I × 3 as the mask covering) and I × 3/M × 1/I × 1 (with I × 3 as the outer layer of a 3-ply mask) were tested. As shown in Fig. 1a(i,ii), no significant difference in overall filtration efficiency was observed from I × 3/3-ply mask and I × 3/M × 1/I × 1, compared to a middle layer only (M × 1) or a 3-ply mask (O × 1/M × 1/I × 1). This is due to the predominant role of the middle layer in particle capturing efficiency (GLM, $P = 0.3033$ for M × 1, I × 3/3-ply, and I × 3/M × 1/I × 1, $P = 0.0023$ for 3-ply mask, I × 3/3-ply mask, and I × 3/M × 1/I × 1 from Fig. 1a(i) and $P = 0.1155$ for M × 1, I × 3/3-ply, and I × 3/M × 1/I × 1, $P = 0.0729$ for 3-ply mask, I × 3/3-ply mask, and I × 3/M × 1/I × 1 from Fig. 1a(ii)). However, it is important to note that the stacked SB fabric layer (I × 3) captured more particles when used as a mask covering or outer layer compared to a single SB fabric (O × 1 or I × 1) in a traditional 3-ply mask.

Interestingly, the filtration efficiency against NaCl aerosols exhibited a biphasic trend: an initial rapid decrease of filtration efficiency up to 0.3–0.75 μm (first phase), followed by a gradual increase with particle size (second phase) (see Fig. 1b(i,ii) for a detailed view). Furthermore, it is evident that an increase in the number of stacked inner layers led to higher filtration efficiency, as observed in Fig. 1a(i). Given that most viruses (<0.4 μm) and bacteria (<5 μm) fall within this size range, this data suggests that employing a stack of inner spunbond PP fabrics as the outermost layer of a mask or mask covering can effectively enhance mask protection against respiratory diseases by reducing the viral/bacterial load on the middle MB layer.[25] In contrast to NaCl aerosols, there was no noticeable biphasic behavior in size dependent filtration efficiency against DOP aerosols (compare Fig. 1b with 1c). However, filtration efficiency was observed to increase with particle size >1 μm (Fig. 1c). Consequently, the filtration efficiency of three stacked inner layers (I × 3) was measured at 23 ± 15% and 85 ± 31% for 2 and 3 μm DOP aerosols, respectively. The overall filtration efficiency data for NaCl and DOP aerosols demonstrate that stacked SB fabrics enhance filtration performance. These fabrics are effective in filtering biological infectious contaminants of all sizes (Fig. 1b) and non-charged larger contaminants (>1 μm; Fig. 1c).

Based on the size dependent filtration mechanisms, the initial high filtration efficiency at the first phase in Fig. 1b can be explained by electrostatic attraction between NaCl aerosols and the spunbond fibers as electrostatic attraction is dominant filtration mechanism for small particles (<300 nm). The decrease in filtration efficiency during the initial phase as particle size increases might be due to the factors such as rise in aerodynamic drag and face velocity, which reduces the potency of electrostatic attraction.[26–29] However, during the second phase, physical mechanisms such as interception, diffusion, sedimentation, and inertial impaction becomes the dominant factors influencing filtration efficiency, leading to an increase in filtration efficiency as the particle size increases (>1 μm). This phenomenon clarifies the particle capturing behavior observed in the stacked inner layers depicted in Fig. 1b. On the other hand, it is reasonable to assume that the non-charged hydrophobic nature of DOP does not exhibit electrostatic attraction with fibers, leading to the disappearance of biphasic filtration efficiency behavior (Fig. 1c). The higher filtration efficiency observed in tests with increasing DOP aerosol sizes, compared to NaCl aerosols, is likely related to the hydrophobic properties of masks that repel water particles and attract oil particles.[30] Similar trends were also observed in the particle size-dependent filtration efficiency of the MB PP middle layer (Fig. S1a†). While the filtration efficiency against 5% NaCl aerosols remained above 86%, it decreased to 59% with DOP aerosols, possibly due to the absence of charge in DOP (compare Fig. S1a(i) with (ii)†). Also, the single SB outer layer showed higher filtration efficiency when tested with DOP than with NaCl aerosols, indicating hydrophobic interaction between hydrophobic fabrics and DOP (Fig. S1b†) (GLM, $P < 0.0001$).

Breathability of various architectures was tested by measuring pressure drop under the same test conditions (Fig. 1d). The overall trend aligns with filtration efficiency, wherein the middle layer exhibits the highest pressure drop (35 ± 1.1 Pa cm^{-2}) compared to other single layers (O: 2 ± 0.5 Pa cm^{-2} and I: 1 ± 0.1 Pa cm^{-2}). The increased pressure drop of the MB middle layer is attributed to its smaller pore size and increased fiber diameter compared to SB fabrics used in the outer and inner layers.[31] Additionally, the pressure drop was observed to rise with the increasing number of stacked inner layers (GLM, $P < 0.0001$): I × 2 (3.9 ± 0.5 Pa cm^{-2}), I × 3 (6.0 ± 0.1 Pa cm^{-2}), I × 4 (7.9 ± 0.6 Pa cm^{-2}), and I × 5 (10.5 ± 1.0 Pa

cm^{-2}). However, it is important to note that the utilization of stacked inner layers as a cover atop a 3-ply mask (*i.e.*, I × 3/3-ply mask) or as an outer layer of a 3-ply mask (*i.e.*, I × 3/M × 1/I × 1) does not surpass the pressure drop limit of 50 Pa cm^{-2}. This underscores the flexibility of stacked inner layers in the design and fabrication of respiratory devices while adhering to differential pressure guidelines (see Table S1†).

2.2 Performance of salt-coated stacked spunbond (SB) fabrics

To evaluate the filter performance of salt-coated SB PP fabrics, filtration efficiency and breathability were characterized at the same testing conditions as in Section 2.1. For this purpose, three different types of salts (NaCl, KCl, K_2SO_4) with different amounts of salts (NaCl: 5, 9, and 13 mg cm^2; KCl: 5 and 9 mg cm^2; K_2SO_4: 5 mg cm^{-2}) were coated onto the three stacked SB inner membranes. Additionally, to evaluate the effect of surfactant in the salt coating formulation, SB inner layers treated with Tween 20 (T20) were also examined. As shown in Fig. 2a(i), salt-coated SB fabrics exhibited overall filtration efficiency ranging from 3% to 5% against NaCl aerosols, which was lower than the efficiency of three stacked SB inner layers without salt coating (I × 3: 21 ± 4%) (one-way ANOVA, $P < 0.0001$). However, the difference in filtration efficiency was less significant in tests with DOP aerosols (Fig. 2a(ii)) (one-way ANOVA, $P = 0.1107$). The underlying reason for these differences was explored by examining the particle size-dependent filtration efficiency. As shown in Fig. 2b(i), I_{NaCl} × 3 showed lower filtration efficiency against small particles (≤0.3 μm) compared to I × 3 (GLM, $P < 0.0001$). Given that the primary mechanism of filtration efficiency at ≤0.3 μm is electrostatic attraction and that both bare and salt-coated SB fabrics have similar pore sizes, the decrease in filtration efficiency against NaCl aerosols can be attributed to the lack of charge in the salt-coated stacked SB fabrics (see Fig. 2b(i) for NaCl and Fig. S2a–c(i)† for KCl and K_2SO_4). However, when testing with non-charged DOP aerosols, both I × 3 and I_{NaCl} × 3 exhibited similar particle-size dependent filtration efficiency trends, with no significant capturing efficiency for particles ≤0.3 μm, regardless of type of salts (see Fig. 2b(ii) for NaCl and Fig. S2a–c(ii)† for KCl and K_2SO_4). Notably, the low filtration efficiency against ≤0.3 μm sized NaCl particles, was also evident in Tween 20 (T20)-treated filters (I_{T20} × 3), demonstrating that the surfactant itself also degrades the electric charge or dipoles of the SB fabrics. The ether groups in polyoxyethylene chains can form hydrogen bonds with water molecules, which contributes to the high solubility of T20 in water.[32] When T20 comes into contact with electret filters, these polyoxyethylene chains can enhance the adsorption of water molecules, which neutralize the electrostatic charges on the electret fibers due to their high dielectric constant.[17]

Considering that the salt coating formulation includes a surfactant, it is plausible that the previously observed filtration efficiency of the salt-coated inner layers could also be attributed to the presence of T20, which is also added to enhance the salt coating. As indicated in Fig. 2c, no noticeable difference was observed in pressure drop between I × 3 and I_{salt} × 3, when compare mean values ranging from 5–8 Pa cm^{-2} across all the conditions tested in this study. This consideration aligns with the maximum allowable differential pressure (50/60/60 Pa cm^{-2}) specified in the ASTM F2100-19e1 standard. The observed trend was consistent regardless of the type of salt (NaCl, KCl, and K_2SO_4) or the quantity of salt used to produce salt-coated antimicrobial PP fabrics (5 mg cm^{-2}, 9 mg cm^{-2}, and 13 mg cm^{-2}). Consequently, stacking salt-coated SB fabrics does not lead to a noticeable decrease in breathability, which is a common concern associated with filter functionalization.

2.3 Application of stacked salt-coated SB fabrics to a mask cover and outer layer of a mask for antimicrobial face masks

Mask performance has been tested by employing NaCl-coated SB fabrics and bare SB fabrics either as a cover over a conventional 3-ply mask (stacking sequence: I_{NaCl} × 3 (cover)/O × 1/M × 1/I × 1, Fig. 3) or as an outer layer of a 3-ply mask (stacking sequence: I_{NaCl} × 3 (outer layer)/M × 1/I × 1, Fig. S3†). As shown in Fig. 3a, the filtration efficiency of a salt-coated mask cover was 2–5% higher than a conventional 3-ply mask (O × 1/M × 1/I × 1), regardless of the aerosol type used in testing (i: NaCl, ii: DOP). However, no significant difference in filtration efficiency was observed between I × 3/3-ply masks (*i.e.*, a stack of three bare inner SB fabrics on top of a 3-ply mask) and I_{NaCl} × 3/3-ply masks (one-way ANOVA, $P = 0.2653$ for Fig. 3a(i) and $P = 0.0652$ for Fig. 3a(ii)). When the outer layer was replaced with three stacked SB fabric (I_{NaCl} × 3/M × 1/I × 1), the filtration efficiency was similar to that observed with the mask cover (*i.e.*, I × 3/O × 1/M × 1/I × 1 and I_{NaCl} × 3/O × 1/M × 1/I × 1; Fig. S3†). Also, particle-size dependent filtration efficiency measurements indicate that the previously observed filtration efficiency decrease at ≤0.3 μm for 5% NaCl particles was no longer evident, regardless of salt quantity and stacking sequence (Fig. 3b and S3b†). This is presumed to be due to the high filtration efficiency of the MB middle layer (Fig. S1a†), which reduces the effects of other layers on overall filtration efficiency performance. Similarly, when tested with DOP aerosols, a progressive rise in filtration efficiency with particle size was observed across all mask structures using stacked SB fabrics, w/ and w/o salt coating (refer to Fig. 3c and S3c†).

The use of the I_{NaCl} × 3 as a cover on top of a 3-ply mask (Fig. 3d) and replacement for the outer layer of a 3-ply mask (Fig. S3d†) resulted in an increase in pressure drop up by 9–10 and 7–9 Pa cm^{-2}, respectively, compared to the conventional 3-ply mask. Importantly, both configurations, regardless of the amount of coated salt, adhered to the ASTM F2100-19e1 guidelines, which specify a differential pressure below 50 Pa cm^{-2} for Level I masks and ≤60 Pa cm^{-2} for Level II and III masks (Fig. 3d and S3d†). Taken together, these findings indicate that when salt-coated SB fabrics are used as a mask cover and an outer layer of a mask, they achieve high filtration efficiency, effectively addressing the limitations observed with salt-coated fabrics alone against small aerosols, and breathability by maintaining pathogen inactivation functionality. As such, it is anticipated that mask configurations incorporating salt-coated

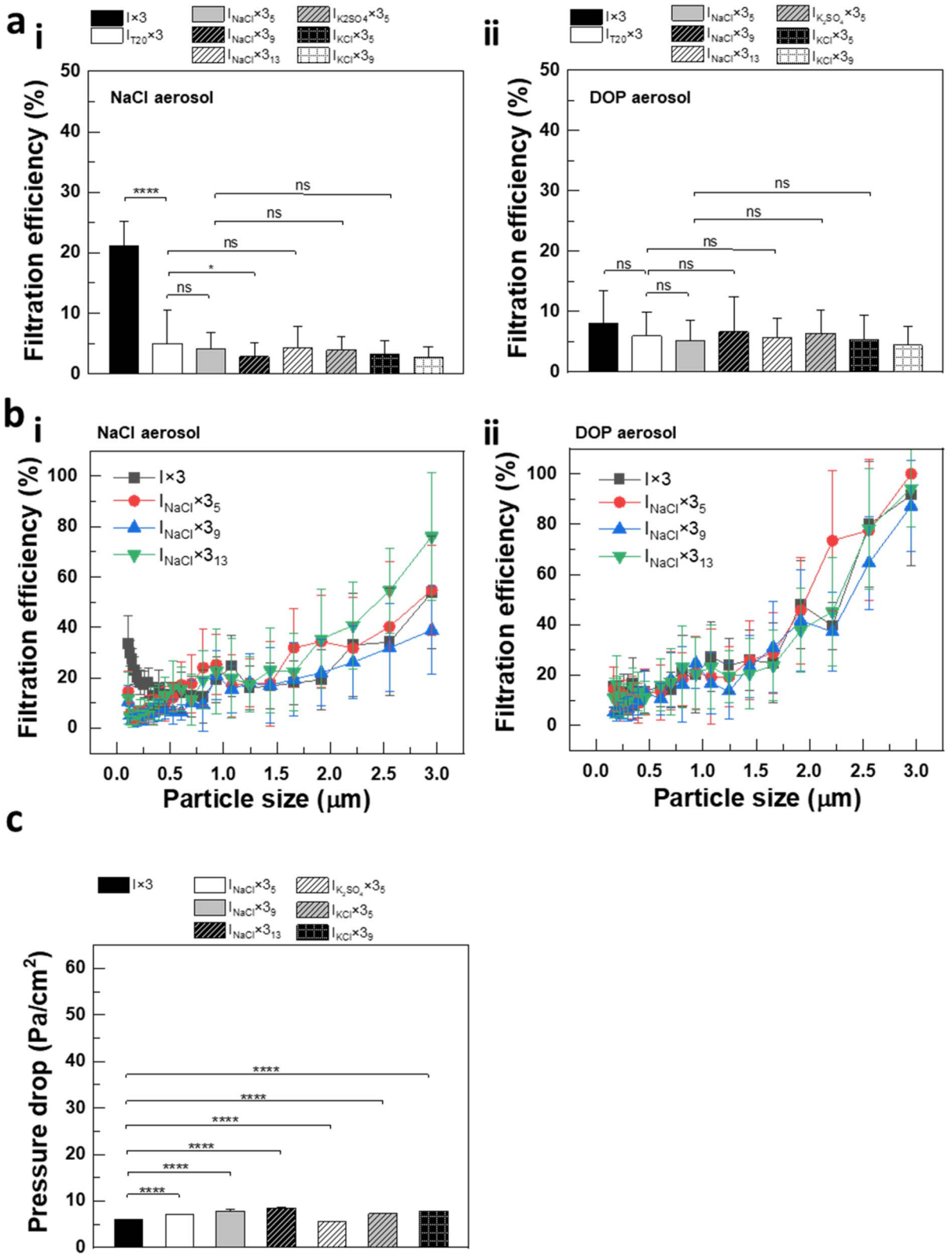

Fig. 2 Filter performance of salt-coated fabrics. Filtration efficiency and breathability were performed according to NIOSH 42CFR84 and ASTM F2100-19e1 standards, respectively. (a and b) Overall filtration efficiency (a) and particle size-dependent filtration efficiency (b) of salt-coated fabrics tested with 5% NaCl aerosol (i) and DOP aerosol (ii). (n = 13–23 for a(i), n = 12–22 for a(ii), n = 9–21 for b(i), and n = 8–24 for b(ii), mean ± SD). (c) Breathability of different conditions of salt-coated fabrics. (n = 10–15, mean ± SD). For all panels: ns, $P > 0.05$; *, $P < 0.05$ and ****, $P < 0.0001$ by one-way ANOVA.

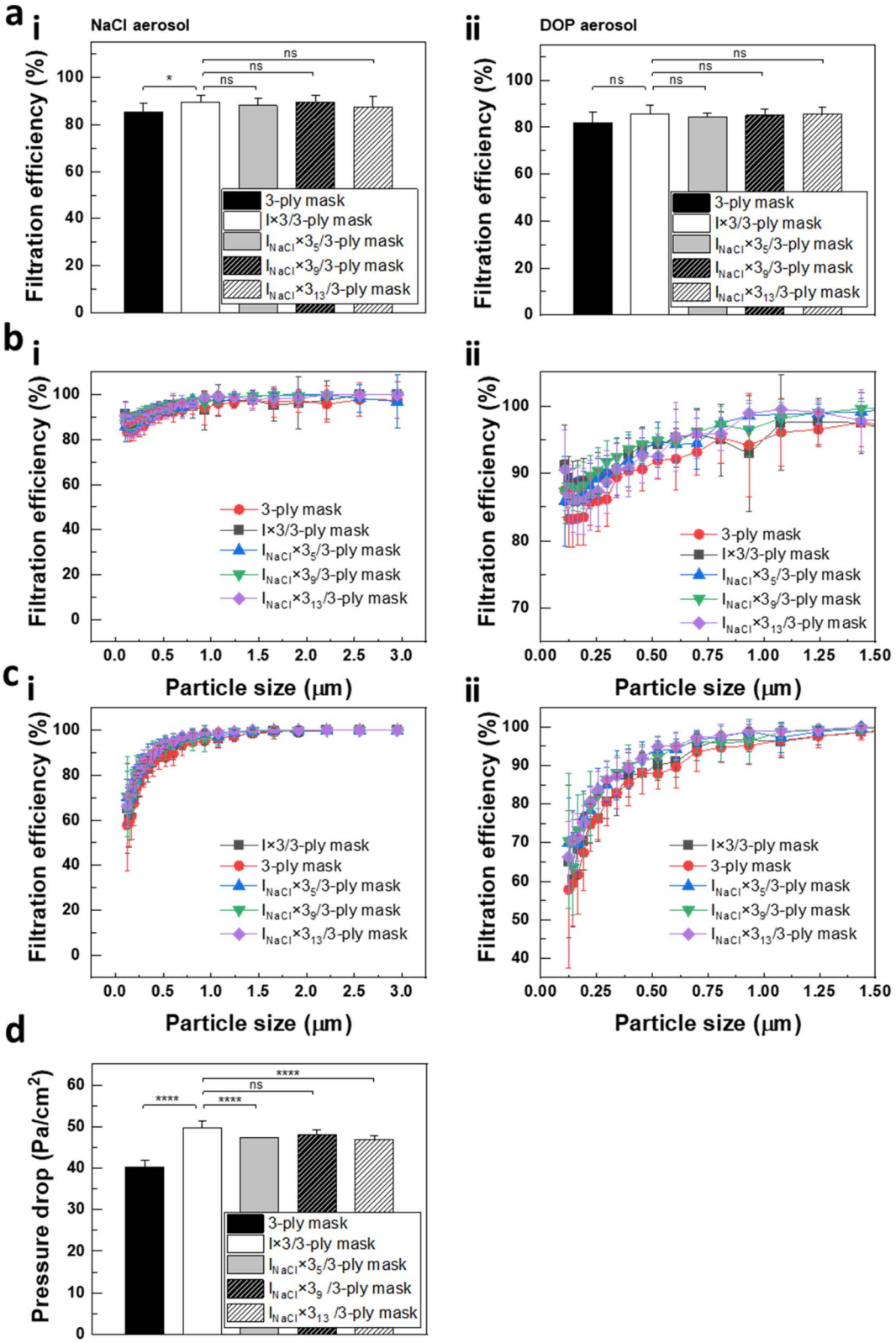

Fig. 3 Filter performance of bare and salt-coated fabrics with different stacking sequences. Filtration efficiency and breathability were performed according to NIOSH 42CFR84 and ASTM F2100-19e1 standards, respectively. (a) Overall filtration efficiency of I × 3 and I_{NaCl} × 3 as a cover of the 3-ply mask (i: 5% NaCl aerosol and ii: DOP aerosol). (n = 10–20 for a(i) and n = 10–15 for a(ii), mean ± SD) (b and c) particle size-dependent filtration efficiency of I × 3 and I_{NaCl} × 3 as cover of the 3-ply mask, tested with 5% NaCl aerosol (b) and DOP aerosol (c) (i: filtration efficiency of stacked fabrics and ii: zoomed-in filtration efficiency of the stacked fabrics). (n = 10–20 for b and n = 10–15 for c, mean ± SD). (d) Breathability of I × 3 and I_{NaCl} × 3 used as an outer. (n = 9–12, mean ± SD). For all panels: ns, $P > 0.05$; *, $P < 0.05$ and ****, $P < 0.0001$ by one-way ANOVA.

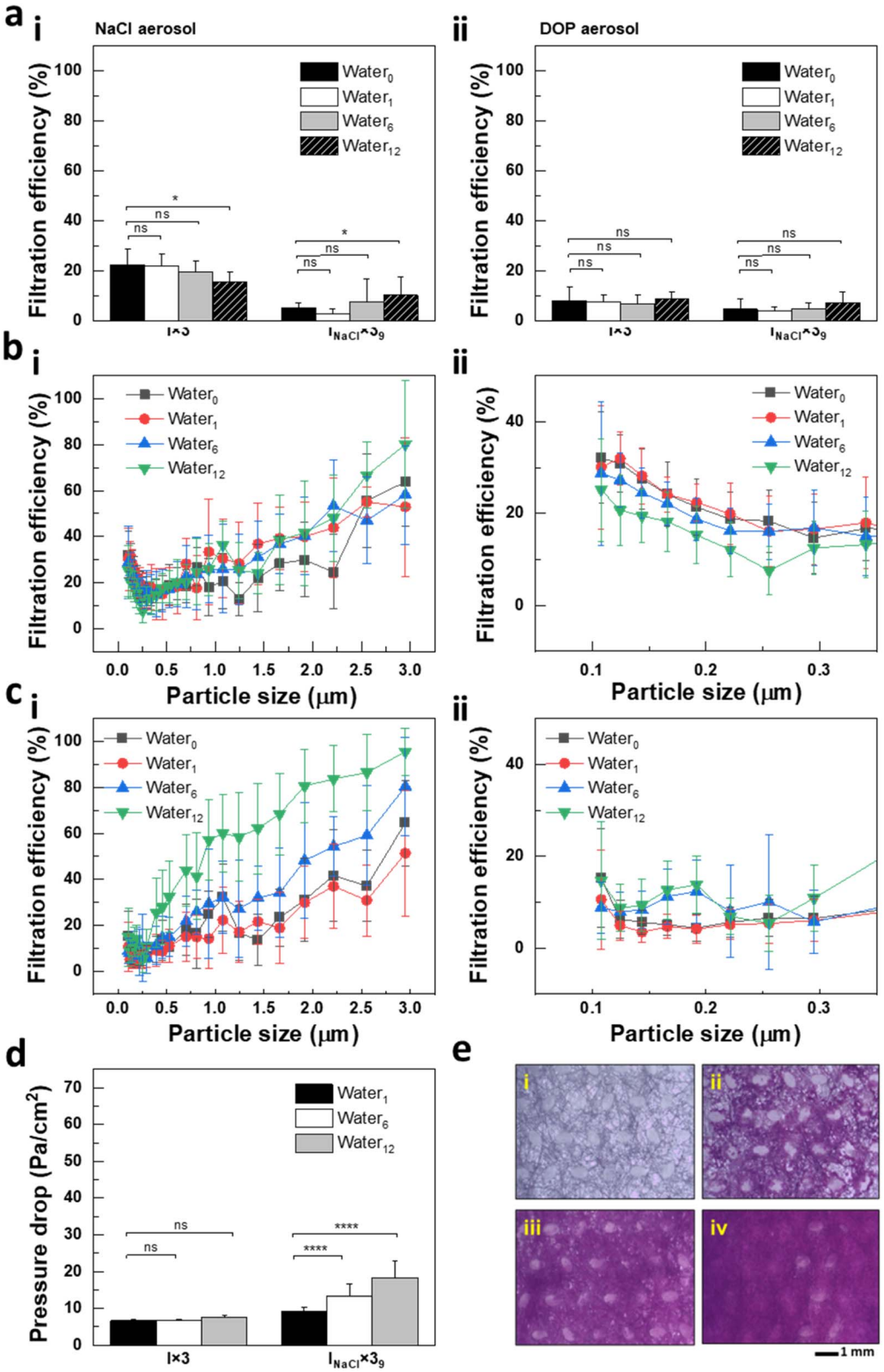

Fig. 4 Filter performance of bare and salt-coated fabrics with different wetness. The wetness of the samples was measured by weighing the samples before and after water spray, followed by dividing the values by mask surface area. Filtration efficiency and breathability were performed according to NIOSH 42CFR84 and ASTM F2100-19e1 standards, respectively. (a) Overall filtration efficiency tested with 5% NaCl (i) and DOP aerosols (ii). ($n = 9$–14 for a(i) and 17–29 for a(ii), mean ± SD). (b and c) Particle size-dependent filtration efficiency of wet I × 3 (b) and wet $I_{NaCl} \times 3_9$, tested with 5% NaCl aerosols (i: filtration efficiency of fabrics and ii: zoomed-in filtration efficiency of the fabrics). ($n = 7$–29 for b and 6–29 for c, mean ± SD). (d) Breathability of wet I × 3 and $I_{NaCl} \times 3_9$ ($n = 9$–14, mean ± SD). Fabrics sprayed with water were labeled $Water_{number}$, with "number" indicating the water amount sprayed (0, 1, 6, 12 mg cm^{-2}). (e) The optical microscope images of wet fabrics. Characterization of $I_{NaCl} \times$

stacked SB fabrics (*e.g.*, I_{salt} × 3/3-ply mask or I_{salt} × 3/M × 1/I × 1) would offer the combined benefits of conventional masks (*e.g.*, high filtration efficiency across all particle sizes due to the presence of MB middle layer) and those of salt-coated fabrics (*e.g.*, rapid pathogen inactivation, reusability, and no concerns over contact transmission).

2.4 Filter performance of three-layered salt-coated SB fabrics in wet conditions

One concern regarding the use of salt coatings is their stability in humid environments. To assess the impact of wetness on filter performance, both I × 3 and I_{NaCl} × 3_9 were exposed to varying amounts of water spray (1, 6, and 12 mg H_2O/cm^2). The level of wetness was modulated by measuring the weight of the filter before and after water spray. As shown in Fig. 4a(i), the overall filtration efficiency of I × 3 fabrics decreased with increasing amount of water sprayed (one-way ANOVA, P = 0.0044). This observation suggests that bare SB PP fabric(s) may be less efficient in capturing infectious particles transported by aqueous mediums (*i.e.*, aerosols, droplets, and splashes) in wet conditions, consistent with prior findings.[33] In contrast, for salt-coated fabrics (I_{NaCl} × 3_9), the mean filtration efficiency appeared to increase with greater wetting (one-way ANOVA, P = 0.0047). When tested with DOP aerosols, wetting did not adversely impact the overall filtration efficiency of both bare and salt-coated fabrics (Fig. 4a(ii)).

Particle-size dependent filtration efficiency was further characterized for I × 3 and wet I_{NaCl} × 3_9 under various wetting conditions. For I × 3 fabrics, filtration efficiency against 5% NaCl aerosols exhibited a biphasic behavior, initially decreasing followed by a gradual increase with particle size (Fig. 4b). For aerosols <0.3 μm, filtration efficiency appeared to decrease as wetness increases (GLM, P < 0.0001). Conversely, the stack of salt-coated SB fabrics (*i.e.*, I_{NaCl} × 3_9) showed a rapid increase in the filtration efficiency against NaCl aerosols as wetness increases (at size >0.3 μm; GLM, P > 0.0001) (Fig. 4c). This indicates that salt-coated fabrics can effectively capture larger infectious contaminants. In comparison to NaCl aerosols, no biphasic behavior of particle-size dependent filtration efficiency was observed for DOP aerosols (see Fig. S4a†). Although filtration efficiency increased rapidly with DOP aerosol size, the stacked SB fabrics without salt coating did not exhibit a significant effect of wetness on capturing efficiency (Fig. S4a†). However, similar to the tests with NaCl aerosols (Fig. 4c), higher filtration efficiency was detected for the salt-coated SB fabric stack (*i.e.*, I_{NaCl} × 3_9) against DOP aerosols (see Fig. 4c for NaCl aerosols and Fig. S4b† for DOP aerosols). This implies that salt-coated filters may effectively capture large particles regardless of their charge characteristics under wet conditions. It is also worth noting that wetting of the salt-coated SB fabrics increases the pressure drop (GLM, P < 0.0001, Fig. 4d). This effect could be attributed to the hydrophilicity of salts, facilitating the formation of a water film around fibers upon wetting (refer to Fig. 4e for optical microscope images before and after spraying sulforhodamine B solution onto I_{NaCl} × 3_9 fabrics). Therefore, under wet conditions, salt-coated fabrics yield two conflicting results: the positive effect of effectively capturing relatively large aerosols and the negative effect of reducing breathability. However, the pressure drop results of wet I_{NaCl} × 3_9 (9–18 Pa cm^{-2}) are still within the standard values mentioned in Table S1.†

The filtration efficiency behavior of I × 3 and I_{NaCl} × 3 as a cover and an outer was also analyzed, as shown in Fig. S5.† No wetness-dependent filtration efficiency behavior was observed under any testing conditions, including 3-ply mask, I × 3/3-ply mask, I_{NaCl} × 3_9/3-ply mask, I × 3/M × 1/I × 1, and I_{NaCl} × 3_9/M × 1/I × 1 (Fig. S5a†). Besides, their particle size-dependent filtration efficiency showed similar values across all different particle sizes (Fig. S5b–d†). This is because the MB middle layer has a high filtration efficiency (Fig. S1a†), which minimizes the impact of the other layers on overall filtration efficiency.

2.5 Filter performance of N95 respirator-only and when combined with I × 3 and I_{NaCl} × 3_9 as a cover

After evaluating the use of salt-coated SB fabrics as a cover and an outer layer for the 3-ply mask, their applicability to N95 respirators was assessed using I_{NaCl} × 3_9. For the breathability analysis of N95 respirators, it's important to note that differential pressure values are not normalized by surface area, unlike surgical masks (Pa cm^{-2}). Therefore, for N95 respirators, the pressure is measured in Pa without surface area adjustment.[34–36] As illustrated in Fig. 5a, an increase in pressure drop was observed when I_{NaCl} × 3_9 was used as a cover: inhalation (N95: 102 ± 5 Pa, I × 3/N95: 124 ± 6 Pa, and I_{NaCl} × 3_9/N95: 138 ± 5 Pa) and exhalation (N95: 114 ± 4 Pa, I × 3/N95: 123 ± 6 Pa, and I_{NaCl} × 3_9/N95: 139 ± 4 Pa). As noted in Fig. 1d and 2c, employing stacked SB fabrics w/ and w/o salt coating over N95 respirator may result in a slight reduction in breathability. However, according to the NIOSH 42CFR84 standard, the differential pressure should not exceed 343 Pa for inhalation and 245 Pa for exhalation airflow. The observed pressure increase when applying stacked SB fabrics to N95 respirators remains within the acceptable range. In terms of particle capturing capacity, all conditions achieved remarkably high filtration efficiency, surpassing 98% (Fig. 5b). This high filtration efficiency was further supported by particle size-dependent filtration efficiency tests, where all values were above 98% (Fig. 5c). Similar to the 3-ply mask, a slightly lower filtration efficiency for small DOP particles (≤0.3 μm) was followed by a rapid increase with an increase in particle size (refer to Fig. 3c for the 3-ply mask and Fig. 5c(ii) for the N95 respirator).

In this work, we observed that a stack of salt-coated SB fabrics exhibited notably high particle-capturing efficiency for aerosols larger than 0.3 μm compared to a single layer of SB

3_9 fabrics after spraying DI water for the measurement of effects of wetness on filtration efficiency. Sulforhodamine B was used to visualize the wetness of fabrics in the images; however, for filtration efficiency and breathability tests, DI water was used. (i–iv) Different amount of DI water was sprayed: (i) 0 mg cm^{-2}, (ii) 1 mg cm^{-2}, (iii) 6 mg cm^{-2} and (iv) 12 mg cm^{-2}. For all panels: ns, P > 0.05; *, P < 0.05 and ****, P < 0.0001 by GLM.

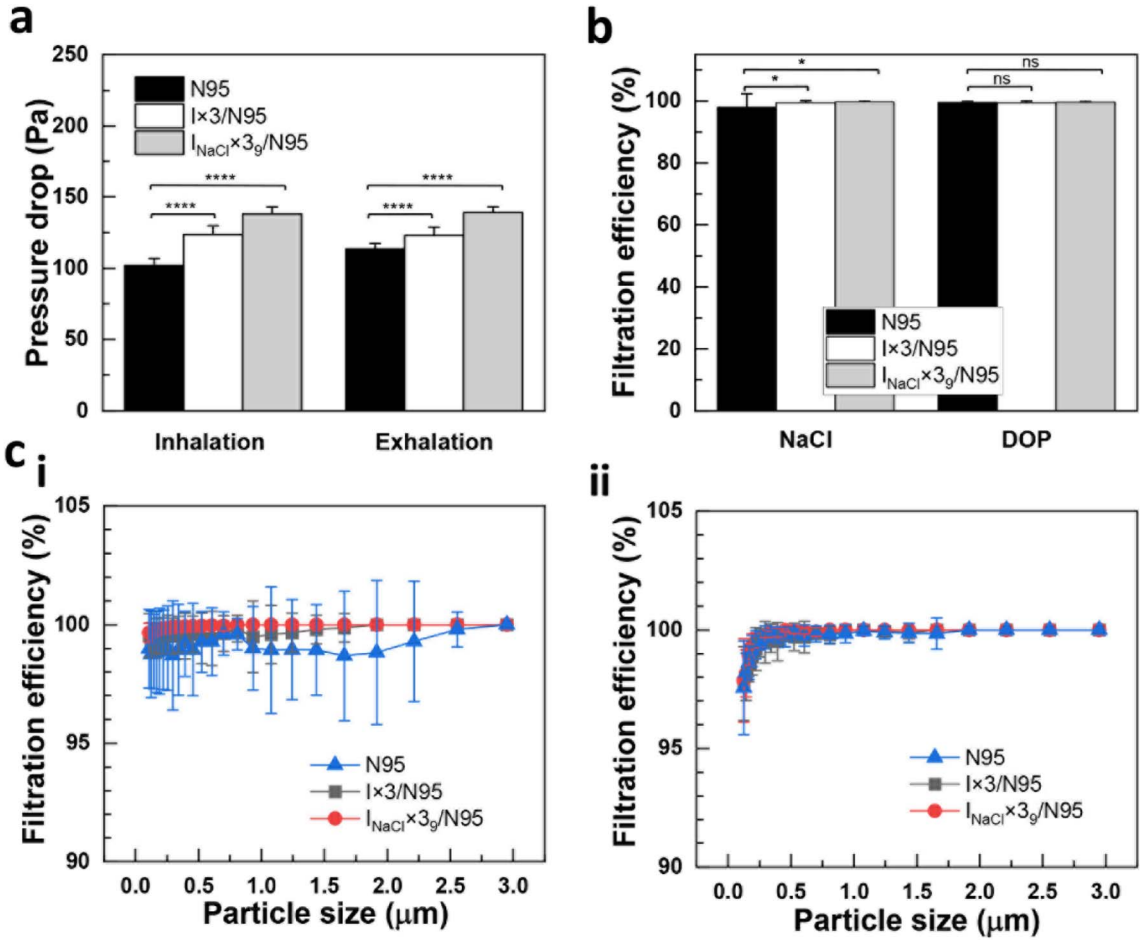

Fig. 5 Filter performance of N95 respirators. Filtration efficiency and breathability were performed according to NIOSH 42CFR84. (a and b) N95 respirators alone, and with I × 3 and $I_{NaCl} \times 3_g$ as a cover of N95. (a: breathability and b: overall filtration efficiency) ($n = 10–15$ for a and $n = 11–18$ for b, mean ± SD). (c) Particle size-dependent filtration efficiency tested with 5% NaCl aerosols (i) and DOP aerosols ($n = 15–19$ for c(i) and $n = 10–18$ for c(ii), mean ± SD) (ii). For all panels: ns, $P > 0.05$; *, $P < 0.05$ and ****, $P < 0.0001$ by GLM.

fabric as the outermost layer of the mask. Filtration efficiency correspondingly increased with particle size. This dual functionality of the salt-coated stacked SB fabric layer—antimicrobial action against pathogens and enhanced particle capture—while effectively managing breathability, significantly contributes to disease transmission prevention.

These findings suggest that stacked salt-coated SB fabrics could effectively replace the outermost layer in existing mask structures, capturing more infectious particles at the surface and neutralizing them with the salt coating. This approach could prolong the mask's performance by reducing contamination burdens on the MB filter within the mask structure over time. Similarly, the antimicrobial and filtering properties of stacked salt-coated SB fabrics make them suitable as covers for masks or N95 respirators. They act as a pre-screening layer, filtering contaminants and minimizing contamination of the mask or respirator underneath, thus extending their useable lifespan.

The primary challenge in implementing antimicrobial masks using salt-coated fabric lies in the antimicrobial mechanism, which relies on the physical destruction caused by growing salt crystals during the water evaporation process. Consequently, in environments with slow water evaporation rates, such as high humidity conditions, pathogen destruction may be hindered due to delayed salt crystallization. Therefore, there is a pressing need for systematic research to investigate alterations in antimicrobial efficacy and mask performance across different environmental conditions. This research is crucial for developing application-specific designs for antimicrobial face masks based on salt-coated antimicrobial technology.

3. Conclusions

In this study, we conducted performance tests on various mask structures utilizing salt-coated SB fabric. Our experiments encompassed testing mask performance with three different salt types (NaCl, KCl, and K_2SO_4) and varying coated salt amounts (5, 9, and 13 mg cm^{-2}), including assessments under wet conditions. Specifically, we evaluated the efficacy of layering multiple salt-coated SB fabrics to potentially replace the single SB fabric typically used as the outermost layer of a mask, or to serve as a cover for existing masks or N95 respirators. Our findings demonstrate that a stack of salt-coated SB fabrics can

maintain a high level of filtration efficiency and breathability when employed as the outermost layer of a mask or as a cover for a mask or respirator. Notably, the MB filter of the mask effectively compensates for lower filtration efficiency for aerosols smaller than 0.3 μm, while achieving high filtration efficiency for aerosol particles larger than 0.3 μm as the number of SB fabrics stacked increases. Compared to a typical mask structure with a single SB fabric as the outermost layer, a stack of salt-coated SB fabrics captures more particles, thus reducing contamination of the MB filter and extending its lifespan. While further resilience testing and stability verification under diverse environmental conditions are essential, our study underscores the potential of salt coating technology in developing feasible antimicrobial face masks or mask coverings.

4. Experimental

4.1 Preparation of salt-coated fabrics

The preparation of salt-coated spunbond (SB) polypropylene (PP) fabric samples was executed following method detailed in previous studies.[37] The process began with the collection of inner SB layers from surgical masks (Fisherbrand Facemasks; Fisher Scientific, Pittsburgh, PA). For the salt coating, NaCl, KCl, and K_2SO_4 were selected based on their toxicity and solubility.[7] Saline solutions were prepared with deionized (DI) water, filtered through a 0.22 μm pore-size filter (Corning, Tewksbury, MA), to achieve saturated concentrations specific to each salt: 29.03 w/v% for NaCl, 26.31 w/v% for KCl, and 9.72 w/v% for K_2SO_4. The different solubilities of these salts resulted in varying amounts of salt deposition on the fabric, thereby limiting the maximum possible coating. Following this, the inner SB fabric layers were immersed in these saline solutions. The fabrics were gently scrubbed to ensure the elimination of any trapped air bubbles, facilitating an even coating. The volume of saline solution absorbed by the fabrics was adjusted by applying vacuum pressure. Fabrics coated with 5 mg cm^{-2} of K_2SO_4, 9 mg cm^{-2} of KCl, and 13 mg cm^{-2} of NaCl were produced by applying a vacuum (5 inHg). Similarly, a vacuum of 8 inHg was applied to achieve 9 mg cm^{-2} of NaCl coating, and 15 inHg was used to obtain 5 mg cm^{-2} of KCl and NaCl. The fabrics were then dried overnight in an incubator (Thermolyne 42000; Dubuque, IA), and the coated fabrics were screened by measuring their weights before and after the coating process. For comparison purpose, SB PP fabrics coated only with Tween 20 (T20) were also prepared by soaking the inner fabrics in DI water containing 1 v/v% T20. The SB fabric was gently scrubbed to release any trapped bubbles and vacuumed at 5 inHg, followed by overnight drying.

The obtained fabrics were labeled as $Fabric_{Coating} \times \#_{Amount}$. In the notation, Fabric specifies the type of PP fabric (inner SB layer (I), middle meltblown (MB) layer (M), or outer SB layer (O)); "Coating" indicates the type of coating material (T20, NaCl, KCl, or K_2SO_4); "#" represents the number of stacked SB PP fabrics (1, 2, 3, 4, or 5); and "Amount" denotes the quantity of salt coating (5, 9, or 13 mg cm^{-2}). Bare fabrics are labeled as "Fabric × #", where "#" is the number of stacked fabrics. The symbol "/" is used to show the arrangement of filter layers, with "A/B" meaning layer A is placed above layer B.

4.2 Wetness test

To analyze the effect of wetness on filter performance, I × 3 and I_{salt} × 3 was sprayed with DI water using a sprayer (Uline, Milton, ON). The amount of sprayed water on the fabric was regulated by weighing the masks before and after spraying with an Explorer Pro balance (Ohaus; Parsippany, NJ). This was followed by calculating the water content per surface area (1, 6, and 12 mg cm^{-2}). The wet filters were then immediately tested for filtration efficiency according to the NIOSH 42CFR84 standard and for breathability following the ASTM F2100-19e1 standards, using the PMFT 1000 (PALAS; Karlsruhe, Germany).

To visually observe the wetness-dependent morphological changes in fabrics, a solution of 1 mM sulforhodamine B (SRB; Sigma-Aldrich) in DI water was sprayed onto salt-coated fabrics. The amount of SRB applied was varied, similar to the above tests, by modulating the volume of the solution sprayed, which was determined by weighing the fabrics before and after spraying. Following this application, the fabrics were characterized through imaging with an optical microscope (Omax G223A-CA; Kent, WA).

4.3 Filtration efficiency and breathability tests

Filtration efficiency and breathability tests of N95 respirators (3 M; Saint Paul, MN) and surgical masks (Fisherbrand Facemasks; Fisher Scientific, Pittsburgh, PA) were performed using the PMFT 1000 (PALAS; Karlsruhe, Germany). The NIOSH 42CFR84 standard, certified by the National Institute for Occupational Safety and Health (NIOSH), was employed for measuring the filtration efficiency of all mask conditions and the breathability of N95 respirators. The NIOSH 42CFR84 filtration efficiency standard necessitates the use of 0.3 μm polydisperse aerosols of 5% NaCl and dioctyl phthalate (DOP) at an airflow rate of 85 L min^{-1}.[34] Masks tested must achieve a minimum efficiency of 95%, 99%, and 99.97% for N95, N99, and N100 respirators, respectively. The NIOSH 42CFR84 breathability standard specifies a maximum resistance of ≤311 Pa at 85 L min^{-1} for inhalation airflow and ≤249 Pa at 85 L min^{-1} for exhalation airflow.[34] Filtration efficiency was calculated by comparing the particle size distribution before and after penetration through the filter, recorded by the Promo LED 2300 (PALAS; Karlsruhe, Germany).

The ASTM F2100-19e1 standards, developed by ASTM International, were utilized for measuring the breathability of surgical masks.[38] This test method classifies surgical/medical masks into Level I, Level II, and Level III, where the maximum differential pressure allowed for Level I masks must be <50 Pa cm^{-2}, and that for both Level II and III masks ≤60 Pa cm^{-2}. The standard specifies the use of an 8 L min^{-1} airflow through 4.9 cm^2 filters, which corresponds to testing a full mask at 163 L min^{-1}.[38] The measured differential pressure (Pa) was normalized to the standard surface area to calculate the pressure (Pa cm^{-2}).

4.4 Statistical analysis

Statistical tests, including the *t*-test, one-way ANOVA and General Linear Model, were conducted using SPSS version 29

(IBM, Armonk, NY, USA). A P value below 0.05 was deemed significant for significance assessments.

Data availability

All data generated or analyzed during this study are included in this published article (and its ESI†).

Author contributions

S. H. performed the experiments, curated the data, and wrote the manuscript; C. M., S. K., E. O. performed experiments, analyzed the data, and edited manuscript; K. H. L. and D.-H. K. provided resources, analyzed data, and edited manuscript; H.-J. C. conceived the experiments, designed the experiments, analyzed the data, provided resources, supervised the research, managed the project, and wrote the manuscript.

Conflicts of interest

H.-J. C is the inventor of salt-coated fabrics and holds a patent for the technology. Nevertheless, the research presented in this study has not been documented elsewhere.

Acknowledgements

The funding for this research was provided by the Natural Sciences and Engineering Research Council of Canada (NSERC) through the Alliance Grant (NSERC AAIA 571019-21 Choi), the NSERC Discovery Grant (RGPIN-2018-04314), the Alberta Innovates Advance Program (AB Innovate ADVANCE 212201119 C), Samsung Electronics Co., Ltd. (IO201216-08204-01), and the National Research Foundation of Korea Brain Pool program (RS-2023-00283369).

References

1 P. Doung-Ngern, R. Suphanchaimat, A. Panjangampatthana, C. Janekrongtham, D. Ruampoom, N. Daochaeng, N. Eungkanit, N. Pisitpayat, N. Srisong and O. Yasopa, Case-control study of use of personal protective measures and risk for SARS-CoV 2 infection, Thailand, *Emerging Infect. Dis.*, 2020, **26**(11), 2607.

2 Y. Wang, H. Tian, L. Zhang, M. Zhang, D. Guo, W. Wu, X. Zhang, G. L. Kan, L. Jia and D. Huo, Reduction of secondary transmission of SARS-CoV-2 in households by face mask use, disinfection and social distancing: a cohort study in Beijing, China, *BMJ Glob. Health*, 2020, **5**(5), e002794.

3 D. C. Payne, S. E. Smith-Jeffcoat, G. Nowak, U. Chukwuma, J. R. Geibe, R. J. Hawkins, J. A. Johnson, N. J. Thornburg, J. Schiffer and Z. Weiner, SARS-CoV-2 infections and serologic responses from a sample of US Navy service members—USS Theodore Roosevelt, April 2020, *Morb. Mortal. Wkly. Rep.*, 2020, **69**(23), 714.

4 D. Lepelletier, B. Grandbastien, S. Romano-Bertrand, S. Aho, C. Chidiac, J. F. Géhanno and F. Chauvin, What face mask for what use in the context of the COVID-19 pandemic? The French guidelines, *J. Hosp. Infect.*, 2020, **105**(3), 414–418.

5 O. O. Fadare and E. D. Okoffo, Covid-19 face masks: a potential source of microplastic fibers in the environment, *Sci. Total Environ.*, 2020, **737**, 140279.

6 S. Kumaran, E. Oh, S. Han and H.-J. Choi, Photopolymerizable, universal antimicrobial coating to produce high-performing, multifunctional face masks, *Nano Lett.*, 2021, **21**(12), 5422–5429.

7 S. Han, E. Oh, E. Keltie, J. S. Kim and H.-J. Choi, Engineering of materials for respiratory protection: salt-coated antimicrobial fabrics for their application in respiratory devices, *Acc. Mater. Res.*, 2022, **3**(3), 297–308.

8 C.-C. Chen and K. Willeke, Aerosol penetration through surgical masks, *Am. J. Infect. Control*, 1992, **20**(4), 177–184.

9 A. Konda, A. Prakash, G. A. Moss, M. Schmoldt, G. D. Grant and S. Guha, Aerosol filtration efficiency of common fabrics used in respiratory cloth masks, *ACS Nano*, 2020, **14**(5), 6339–6347.

10 C. M. Orton, H. E. Symons, B. Moseley, J. Archer, N. A. Watson, K. E. J. Philip, S. Sheikh, B. Saccente-Kennedy, D. Costello and W. J. Browne, A comparison of respiratory particle emission rates at rest and while speaking or exercising, *Commun. Med.*, 2022, **2**(1), 44.

11 X. Xie, Y. Li, H. Sun and L. Liu, Exhaled droplets due to talking and coughing, *J. R. Soc., Interface*, 2009, **6**(suppl_6), S703–S714.

12 W. G. Lindsley, T. A. Pearce, J. B. Hudnall, K. A. Davis, S. M. Davis, M. A. Fisher, R. Khakoo, J. E. Palmer, K. E. Clark and I. Celik, Quantity and size distribution of cough-generated aerosol particles produced by influenza patients during and after illness, *J. Occup. Environ. Hyg.*, 2012, **9**(7), 443–449.

13 S. Asadi, C. D. Cappa, S. Barreda, A. S. Wexler, N. M. Bouvier and W. D. Ristenpart, Efficacy of masks and face coverings in controlling outward aerosol particle emission from expiratory activities, *Sci. Rep.*, 2020, **10**(1), 1–13.

14 E. Mansour, R. Vishinkin, S. Rihet, W. Saliba, F. Fish, P. Sarfati and H. Haick, Measurement of temperature and relative humidity in exhaled breath, *Sens. Actuators, B*, 2020, **304**, 127371.

15 J. W. Cherrie, S. Wang, W. Mueller, C. Wendelboe-Nelson and M. Loh, In-mask temperature and humidity can validate respirator wear-time and indicate lung health status, *J. Exposure Sci. Environ. Epidemiol.*, 2019, **29**(4), 578–583.

16 A.-B. Wang, X. Zhang, L.-J. Gao, T. Zhang, H.-J. Xu and Y.-J. Bi, A review of filtration performance of protective masks, *Int. J. Environ. Res. Public Health*, 2023, **20**(3), 2346.

17 J. Lee and J. Kim, Material properties influencing the charge decay of electret filters and their impact on filtration performance, *Polymers*, 2020, **12**(3), 721.

18 E. Hossain, S. Bhadra, H. Jain, S. Das, A. Bhattacharya, S. Ghosh and D. Levine, Recharging and rejuvenation of decontaminated N95 masks, *Phys. Fluids*, 2020, **32**(9), 093304.

19 A. M. Grillet, M. B. Nemer, S. Storch, A. L. Sanchez, E. S. Piekos, J. Leonard, I. Hurwitz and D. J. Perkins, COVID-19 global pandemic planning: performance and electret charge of N95 respirators after recommended decontamination methods, *Exp. Biol. Med.*, 2021, **246**(6), 740–748.

20 H. Saleem and S. J. Zaidi, Sustainable use of nanomaterials in textiles and their environmental impact, *Materials*, 2020, **13**(22), 5134.

21 S. Rengasamy, E. Fisher and R. E. Shaffer, Evaluation of the survivability of MS2 viral aerosols deposited on filtering face piece respirator samples incorporating antimicrobial technologies, *Am. J. Infect. Control*, 2010, **38**(1), 9–17.

22 S. Li, A. Chen, Y. Chen, Y. Yang, Q. Zhang, S. Luo, M. Ye, Y. Zhou, Y. An and W. Huang, Lotus leaf inspired antiadhesive and antibacterial gauze for enhanced infected dermal wound regeneration, *Chem. Eng. J.*, 2020, **402**, 126202.

23 F.-S. Quan, I. Rubino, S.-H. Lee, B. Koch and H.-J. Choi, Universal and reusable virus deactivation system for respiratory protection, *Sci. Rep.*, 2017, **7**(1), 39956.

24 P. Yi, X. Zuo, D. Lang, M. Wu, W. Dong, Q. Chen and L. Zhang, Competitive adsorption of methanol co-solvent and dioctyl phthalate on functionalized graphene sheet: Integrated investigation by molecular dynamics simulations and quantum chemical calculations, *J. Colloid Interface Sci.*, 2022, **605**, 354–363.

25 J. Louten, *Virus Structure and Classification*. Essential Human Virology 2016, vol. 19.

26 M. Rezaei and M. S. Johnson, Airborne Nanoparticles: Control and Detection. *Air Pollution Sources, Statistics and Health Effects*, 2021, pp. 85–133.

27 F. Drewnick, J. Pikmann, F. Fachinger, L. Moormann, F. Sprang and S. Borrmann, Aerosol filtration efficiency of household materials for homemade face masks: Influence of material properties, particle size, particle electrical charge, face velocity, and leaks, *Aerosol Sci. Technol.*, 2021, **55**(1), 63–79.

28 T. Joo, M. Takeuchi, F. Liu, M. P. Rivera, J. Barr, E. S. Blum, E. Parker, J. H. Tipton, J. Varnedoe and B. Dutta, Evaluation of particle filtration efficiency of commercially available materials for homemade face mask usage, *Aerosol Sci. Technol.*, 2021, **55**(8), 930–942.

29 A. M. R. Kabir, D. Inoue, Y. Kishimoto, J.-i. Hotta, K. Sasaki, N. Kitamura, J. P. Gong, H. Mayama and A. Kakugo, Drag force on micron-sized objects with different surface morphologies in a flow with a small Reynolds number, *Polym. J.*, 2015, **47**(8), 564–570.

30 D. Deng, D. P. Prendergast, J. MacFarlane, R. Bagatin, F. Stellacci and P. M. Gschwend, Hydrophobic meshes for oil spill recovery devices, *ACS Appl. Mater. Interfaces*, 2013, **5**(3), 774–781.

31 C. D. Zangmeister, J. G. Radney, M. E. Staymates, E. P. Vicenzi and J. L. Weaver, Hydration of hydrophilic cloth face masks enhances the filtration of nanoparticles, *ACS Appl. Nano Mater.*, 2021, **4**(3), 2694–2701.

32 B. A. Kerwin, Polysorbates 20 and 80 used in the formulation of protein biotherapeutics: structure and degradation pathways, *J. Pharm. Sci.*, 2008, **97**(8), 2924–2935.

33 A. Mahdavi, F. Haghighat, A. Bahloul, C. Brochot and C. Ostiguy, Particle loading time and humidity effects on the efficiency of an N95 filtering facepiece respirator model under constant and inhalation cyclic flows, *Ann. Occup. Hyg.*, 2015, **59**(5), 629–640.

34 National Institute for Occupational Safety and Health, *NIOSH 42CFR84: Respiratory Protective Devices*. U.S. Department of Health and Human Services: Washington, DC, 1995.

35 European Committee for Standardisation, *EN 149: Respiratory Protective Devices–Filtering Half Masks to Protect against Particles–Requirements, Testing, Marking*. CEN: Brussels, Belgium, 2009.

36 Standardization Administration of the People's Republic of China, *GB 2626-2006: Respiratory Protective Equipment–Non-powered Air-Purifying Particle Respirator*, SAC, Beijing, China, 2006.

37 I. Rubino, E. Oh, S. Han, S. Kaleem, A. Hornig, S.-H. Lee, H.-J. Kang, D.-H. Lee, K.-B. Chu and S. Kumaran, Salt coatings functionalize inert membranes into high-performing filters against infectious respiratory diseases, *Sci. Rep.*, 2020, **10**(1), 13875.

38 ASTM International, *ASTM F2100-19e1: Standard Specification for Performance of Materials Used in Medical Face Masks*, ASTM International, West Conshohocken, PA, 2019.